# The Effects of the Variations in Sea Surface Temperature and Atmospheric Stability in the Estimation of Average Wind Speed by SEASAT-SASS

W. TIMOTHY LIU

*Jet Propulsion Laboratory, California Institute of Technology, Pasadena, CA 91109*

(Manuscript received 7 April 1983, in final form 26 September 1983)

ABSTRACT

Wind speeds from the scatterometer (SASS) on the ocean observing satellite SEASAT averaged over 2° latitude by 2° longitude and a 92-day period are compared with wind speeds from ship reports in the western North Atlantic and the eastern North Pacific, where the concentrations of ship reports are high and the ranges of atmospheric stability and sea surface temperature are large. The comparison results are consistent for each region and for the combined data. Scatterometer winds are found to be generally higher than ship winds. The systematic dependences of the difference between scatterometer winds and ship winds on sea surface temperature and atmospheric stability are identified. The quality of ship reports is not ideal but should not depend on atmospheric stability or sea surface temperature. The systematic dependences, therefore, may reflect the characteristics of scatterometer winds.

Multivariate regressions are used to extract the independent effects of different factors on the wind speed differences. The difference between scatterometer winds and neutral winds from ship reports increases with increasing atmospheric stability and the trend is more prominent under stable than unstable conditions. By replacing neutral winds with observed winds, the stability dependence is reduced. At low wind speeds, the wind difference is found to depend also on sea surface temperature, probably due to temperature dependent factors, such as water viscosity, which are not included in the SASS model function. This dependence is greatly reduced at wind speeds higher than 8 m $s^{-1}$. After the systematic dependence is removed from the scatterometer winds, the rms difference between the scatterometer winds and the neutral winds from ship reports was reduced from 1.7 to 0.9 m $s^{-1}$.

The scatterometer measures backscatter from ocean surface short waves. The results of this study call for better understanding of the energy input from the atmosphere to the short waves, which may depend on atmospheric stability and the dissipation of this energy through processes that may be affected by temperature dependent fluid properties (e.g., viscosity and surface tension).

## 1. Introduction

Between launching on 28 June 1978 and failure on 10 October 1978, the ocean observing satellite SEASAT provided about three months of data to study the feasibility of using space-borne microwave sensors to measure ocean surface parameters. The evaluation of the ability of the microwave scatterometer (SASS) to measure near surface wind vectors has been largely limited to midlatitude and mid-ocean experiments, the Joint Air–Sea Interaction (JASIN) experiment and the Gulf of Alaska SEASAT Experiment (GOASEX), which cover only small ranges of environmental conditions. There were concerns that space and time dependent errors in SASS winds, not discovered and corrected in these evaluations, may affect the study of low frequency forcing of ocean circulations by the momentum exchanges from the atmosphere. Brown (1983) and others have cautioned against unqualified application to world oceans of SASS winds tuned to ideal conditions. The objective of this study is mainly to examine the systematic difference between the neutral wind speeds inferred from the measurements of SEASAT-SASS and those derived from ship reports over large ranges of sea surface temperature and atmospheric stability.

The scatterometer beams K-band microwave radiation (14.6 GHz) to the ocean surface and measures the backscatter. The theory describing microwave scatter from a rough surface has been adequately formulated (e.g., Ishimaru, 1978) but the relation between ocean surface roughness and surface wind or stress is not well understood. Over the ocean, the backscatter for near vertical incidence is due to reflection by the mirror-like wavelets. Away from the vertical, the return is governed by resonant scatter from short waves tilted by long waves and the backscatter coefficient, or normalized cross section, $\sigma$, is found to depend not only on wind speed but also on wind direction. Since $\sigma$ is symmetric about the mean wind direction and SASS measures at two azimuth angles, there can be up to four solutions. These multiple solutions yield widely different wind directions but nearly the same wind speed (Boggs, 1982). There have been various attempts to remove the ambiguity in SASS wind direction (e.g., Wurtele *et al.*, 1982) but unambiguous wind directions for the SEASAT data are not yet available. This study will be confined to wind speeds for off-vertical observations.

According to the theory of Bragg scattering (Wright, 1968), $\sigma$ is proportional to the spectral density of short waves. The mechanism of the generation of short waves is not well understood but appears to depend on the near surface wind profile and wave-induced turbulence (Phillips, 1977). It has been postulated that the short waves depend on surface stress (momentum transport) and $\sigma$ can be related uniquely to an equivalent neutral wind (e.g., Jones *et al.*, 1982). The equivalent neutral wind is the wind associated with a given surface stress when the atmosphere is neutrally stratified. The vertical wind speed profile in the atmospheric surface layer (lower 10–50 m of the atmosphere where the stress is approximately constant) depends on stability, which in turn is affected by both temperature and humidity stratification. The equivalent neutral wind is related to the friction velocity $U_*$, which is the square root of the kinematic stress, independent of atmospheric stability. An empirical relation, the model function SASS-1, between $\sigma$ and the equivalent neutral wind at 19.5 m ($U_n$) has been established and used to process all SASS observations (Schroeder *et al.*, 1982). The neutral wind is used instead of the observed wind to eliminate the necessity of including a stability term in the model function.

If the hypothesis that short waves are governed by surface stress is valid, $\sigma$ would correlate better with $U_*$ than the observed wind $U$ (or $U_n$ derived from $U$) when stress and wind are independently obtained. Liu and Large (1981) (hereafter referred to as LL) compared $\sigma$ with more than 80 h of coincident $U_*$ obtained by dissipation method during the JASIN experiment and found that the correlation between $\sigma$ and $U_*$ is no better than that between $\sigma$ and $U_n$ derived from $U$. LL also used these $U_n$ as inputs and evaluated $\sigma$ with the SASS model function. They compared this derived $\sigma$ with those observed by SASS and found that the discrepancy varies with atmospheric stability. The distribution of the data used by LL, however, is uneven with most data at near neutral conditions. An examination of the relation between $U_n$ derived from SASS observations and from *in situ* measurements over a larger range of atmospheric stability was needed.

Atmospheric stability varies with surface wind speed and sea surface temperature $T_s$ (see Section 3). The variation in wind speed may independently affect the accuracy of SASS wind due to incorrectly calibrated model functions but the effects may appear as stability dependence. In addition, wave spectra may depend on water viscosity (Lleonart and Blackman, 1980), which varies with water temperature. Since the SASS model function does not account for such effects, variations in $T_s$ may cause errors in SASS wind independent of atmospheric stability. This effect has yet to be directly demonstrated and isolated from those of stability. Jones *et al.* (1982) compared SASS winds with "surface truth" observed near hurricanes Fico and Ellen and over extratropical storms in areas with, supposedly, quite different $T_s$. However, the uncertainty in the quality of the estimations of surface wind and other factors made the results unreliable as indicators of temperature dependence. Weissman *et al.* (1980) observed changes in L-band radar backscatter at the boundary of the Gulf Stream, at a place of strong sea surface temperature gradient. Insufficiency in *in situ* measurements, however, prevented the isolation of temperature dependence from other effects present such as those from instability induced atmospheric convection as suggested by Thompson *et al.* (1983).

There were no high quality *in situ* measurements covering large ranges of atmospheric stability and sea surface temperature during the SEASAT period. In this study, SASS winds will be compared with winds from ship reports over large areas. Ship winds, due to observation methods, are not good standards for establishing the absolute accuracy of SASS winds as recognized by Pierson (1983) and others. However, there is no reason to believe that the accuracy of ship winds depends on atmospheric stability or sea surface temperature after the effects of wind speed variation are filtered out. Neutral winds, on the other hand, are theoretical quantities that have to be derived from observations through a model of the atmospheric surface layer. Modeling errors may cause the accuracy of neutral winds to depend on stability or sea surface temperature. Therefore, neutral winds from SASS are compared not only with neutral winds from ship reports but also observed winds. A quality selection procedure is designed to increase the quality of ship wind data, and by averaging over 2° latitude by 2° longitude areas and the 92 day period, the random errors will be reduced.

## 2. The ship data

Two regions (Fig. 1) with high concentrations of ship reports and large ranges of atmospheric stability were selected for the study. The first region is in the western N. Atlantic (10–70°N, 280–320°E) and the second is in the eastern North Pacific (10–60°N, 220–260°E). The ship reports used were the ship radio reports collected by the Fleet Numerical Oceanographic Central (FNOC) during the SEASAT period. Four parameters: wind speed $U$, sea surface temperature $T_s$, air temperature $T$, and dew point temperature $T_d$, were extracted from the reports after the application of a quality control procedure. The first step in the quality control procedure was an attempt to remove reports with position and time errors. Data with positions on land were first discarded. The displacement and time elapsed between consecutive reports by the same ship were used to evaluate mean ship speed. When the speed exceeded 35 kt, the second report was

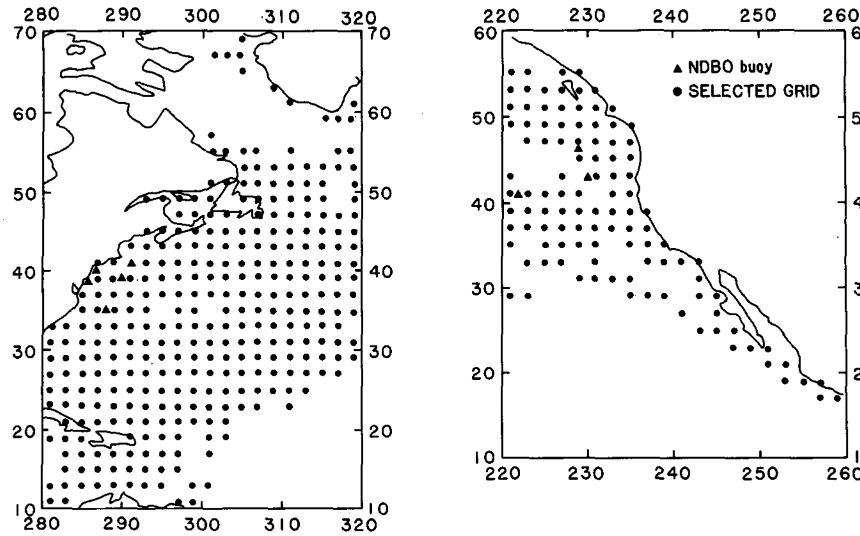


FIG. 1. The areas of study, with the position of selected grids and NDBO buoys.

discarded. The second step removed data outside reasonable ranges. The range set for wind speeds was 0–90 kt; for sea surface temperature it was 0–40°C. The ranges for air temperature and dew point temperature were from −10 to 40°C. In the last step, the mean and standard deviation for each 2° latitude by 2° longitude area and the 92-day period (11 July 1978–10 Oct. 1978) were calculated. Wind speeds outside ±3.56 standard deviations from the mean were discarded (cf Rasmusson and Carpenter, 1982) and a criterion of ±2 standard deviations from the mean was arbitrarily chosen for temperature. All together about 13% of ship reports were discarded.

The measurements of eight moored buoys operated by the National Data Buoy Office, located within the regions of study and reporting during most of the 92-day period were acquired for comparison with ship data. The positions of these buoys are shown in Fig. 1. In Fig. 2, the buoy winds were adjusted to 19.5 m using similarity profiles described in Liu *et al.* (1979) (see Section 3) and averaged over the 92 days. The corresponding ship winds were averaged over the same period and over the 2° areas in which the buoys were situated. The height of the average ship wind was assumed to be the same as the reference height for scatterometer winds, which is 19.5 m. Despite studies showing the influence of ship structures on the accuracies of individual wind measurements (e.g., Ching, 1976), the average ship winds agree remarkably well with the adjusted buoy winds in the limited comparison shown in Fig. 2; the difference is always less than 0.5 m $s^{-1}$.

## 3. Evaluation of average neutral winds

The surface-layer parameterization method of Liu *et al.* (1979) (hereafter referred to as LKB) was used to reduce wind speeds measured at different levels to the reference height of 19.5 m and to evaluate the neutral wind and the stability parameter $\xi = Z/L$ where $Z$ is the height and $L$ is the Obukhov length as formulated by LKB. The Obukhov length is a scaling length representing the balance between turbulent production by shear and by buoyancy. In using this method, $L$ is parameterized in terms of $U$, $T$, $T_d$, and $T_s$ and the velocity profile is linked to the temperature and humidity profiles through $L$. This method of determining $U_n$ (also described in LL) includes the effects of both temperature and humidity stratifications on the wind profile and the different mechanisms in momentum, heat and moisture transports at the interface.

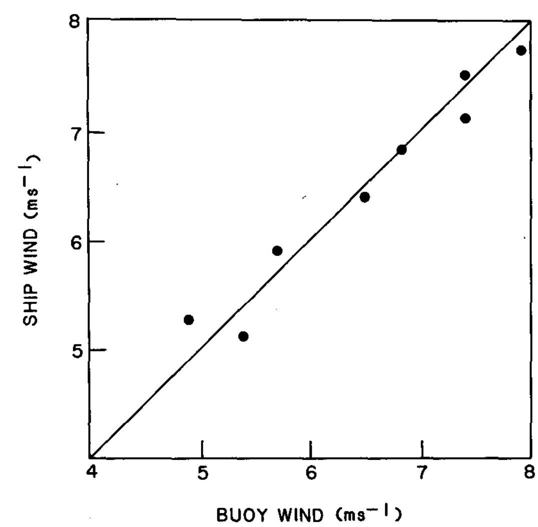


FIG. 2. Comparison of buoy winds adjusted to 19.5 m to ship winds averaged over 2° areas in which the buoy is situated. Both types of winds are averaged over the 92 day period.

With $U$, $T$, $T_d$, $T_s$ and the instrument heights, the universal similarity profiles of wind speeds, temperature and humidity (see LKB) are solved simultaneously to obtain $L$, $U_*$ and the roughness parameter $Z_0$. To determine the actual wind speeds at the reference height $Z_R$, the results are substituted in the velocity profile equation:

$$U = 2.5U_*\left(\ln\left(\frac{Z}{Z_0}\right) - \psi\right),$$

with $Z = Z_R$. In the above equation $\psi$ is a function of $\xi$. For neutral wind, $\psi$ is set to zero and $U$ becomes $U_n$. The dashed line in Fig. 8 (discussed in Section 5) shows how the ratio $U/U_n$ varies with stability according to LKB.

The data contain some strongly stable conditions, with the bulk Richardson number larger than the critical value. The bulk Richardson number is defined as

$$\mathrm{Ri} = gZ(T - T_s)/(\bar{T}U^2)$$

where $g$ is the acceleration due to gravity and $\bar{T}$ is the average temperature in kelvins (K). In such cases, turbulence subsides and there is no valid method to determine $U_n$ or $\xi$. Therefore, a small amount of data with $\mathrm{Ri} > 0.25$ were discarded in this study.

In Fig. 3, two methods of evaluating the average $U_n$ are compared. The 2° areas in the North Atlantic region with more than 50 reports in each of the 4 parameters: $U$, $T$, $T_d$, $T_s$ during the period were used in this comparison. The bulk parameterization method, represented by the operator $F(\;)$, was first applied to each set of parameters to obtain $U_n = F(U, T, T_d, T_s)$ and then all the $U_n$ within each 2° area over the period were averaged to obtain $\bar{U}_n$. In the second method, the four parameters were individually averaged to obtain $\bar{U}$, $\bar{T}$, $\bar{T}_a$, $\bar{T}_s$. Average $\hat{U}_n = F(\bar{U}, \bar{T}, \bar{T}_a, \bar{T}_s)$ were

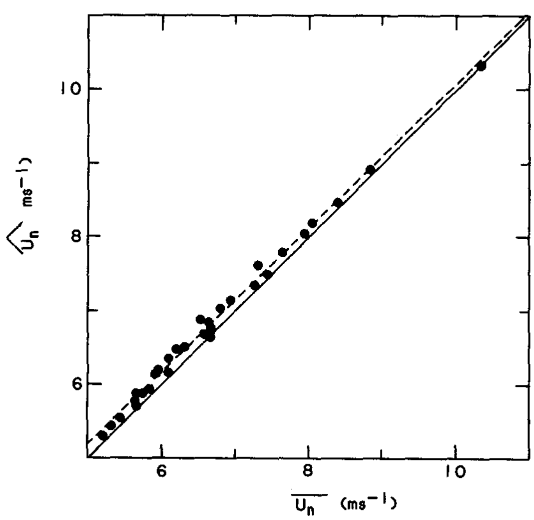


FIG. 3. Comparison of neutral winds from mean parameters $\hat{U}_n$ and the means of neutral winds $\bar{U}$. Solid line is the perfect fit $\hat{U} = \bar{U}$. Broken line is the least square fit of the data.

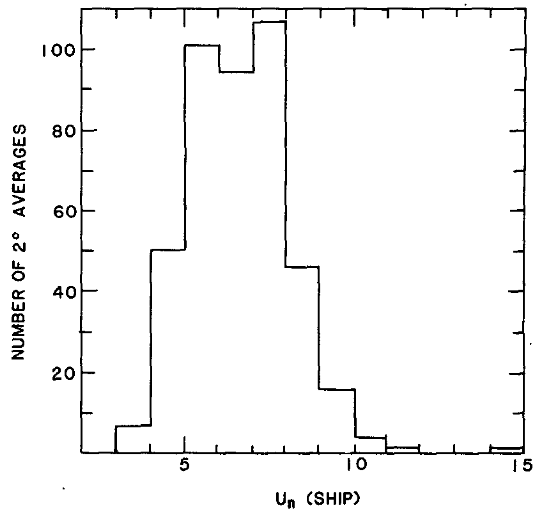


FIG. 4. Histogram of the distribution of averaged neutral wind from ship reports.

then obtained by applying $F$ to these average parameters. The differences between $\bar{U}_n$ and $\hat{U}_n$ shown in Fig. 3 are insignificant. Esbensen and Reynolds (1981) have compared the two methods of time averaging with data from ocean weather stations and Liu and Katsaros (1984) have compared similar methods in spatial averaging using aircraft data during the JASIN experiment. Both studies found the difference between the two averaging methods to be small. In this study, the second method was used to obtain $U_n$ because $T_d$ was often missing from ship reports. Since fluctuations in $T_d$ have much lower frequencies than those in $U$, and $T_d$ affects the determination of $U_n$ only through stability, the theoretical advantage of applying the first method does not justify the sacrifice of a large number of wind reports with corresponding $T_d$ missing. The average height of measurement was assumed to be 19.5 m in evaluating $\hat{U}_n$. In Section 5, the carets are dropped from $U_n$ and $\xi$, and the over-bars from $T_s$ for simplicity.

Only areas with more than 20 wind reports are used in this study. This criterion is chosen as a compromise between increasing accuracy and keeping enough data for meaningful analysis as revealed by the plot of the difference between average SASS wind and average ship wind versus the number of wind reports in the corresponding 2° areas during the 92 days. The positions of the center of these areas are shown in Fig. 1. A histogram showing the distribution of these selected averages $U_n$ (ship) is shown in Fig. 4. Corresponding histogram for the averaged observed winds $U$ (Ship) is very similar and not shown.

## 4. Satellite data

The scatterometer winds are obtained from the "streamlined" SASS data set in the on-line archives of the Pilot Ocean Data System at the Jet Propulsion Laboratory. The data set is the same as that in the Geophysical Data Record (GDR) generated by the SEASAT Project (Boggs, 1982), but with the supporting data deleted. The wind vectors in the GDR are determined by first matching corresponding $\sigma$ from the orthogonal forward and aft beams and then using these values in a least-square inversion of the model function. The model function is the relation

$$\log\sigma = G(\theta, \chi') + H(\theta, \chi')\log U_n,$$

where $\theta$ is the angle between the radar beam and nadir, and $\lambda'$ is the azimuth angle of the beam relative to the mean wind direction. The empirical coefficients $G$ and $H$ are tabulated separately for horizontal and vertical polarization every 2° in $\theta$ and every 10° in $\lambda'$.

The SASS winds available consist of multiple solutions which differ in wind direction but have nearly the same wind speed. To obtain averages, all off-nadir ($\theta > 20°$) solutions that are lower than 35 m s$^{-1}$ and higher than 0 m s$^{-1}$ were used. These average SASS winds over 2° areas and the 92-day period are denoted as $U_n$ (SASS) in this paper. The deviations, $\delta U = U_n$ (SASS) $-$ $U_n$ (ship) and $\delta U' = U_n$ (SASS) $-$ $U$ (ship) do not show any significant dependence on the number of SASS winds averaged. Therefore, all the areas corresponding to those selected for $U_n$ (ship) were used in the analysis.

## 5. Comparison with FNOC ship data

The wind speed differences $\delta U$ and $\delta U'$ are plotted against $U_n$, $T_s$, and $\xi$ from ship reports in Figs. 5–7 averaged according to bands with bandwidths of 2 m s$^{-1}$, 5°C and 0.5 unit (dimensionless), respectively. The standard deviation and the number of data (2° averages) for $\delta U$ in each band are also shown. Those for $\delta U'$ differ only slightly and are not shown. Figs. 5–7 show that the SASS winds are generally higher than wind speeds from ship reports, agreeing with the comparison by Chelton and O'Brien (1982) in the Tropical Pacific. The discrepancies, however, are not confined to tropical regions. For all 428 set of data, the average $\delta U$ is about 1.2 m s$^{-1}$ or 18% of the average $U_n$ and the rms difference between $U_n$ (SASS) and $U_n$ (ship) is 1.7 m s$^{-1}$. Merchant ships tend to avoid storms and the quality control procedure discards extreme data. Thus, ship winds used in this study may have been biased low. Since ship winds compared well with

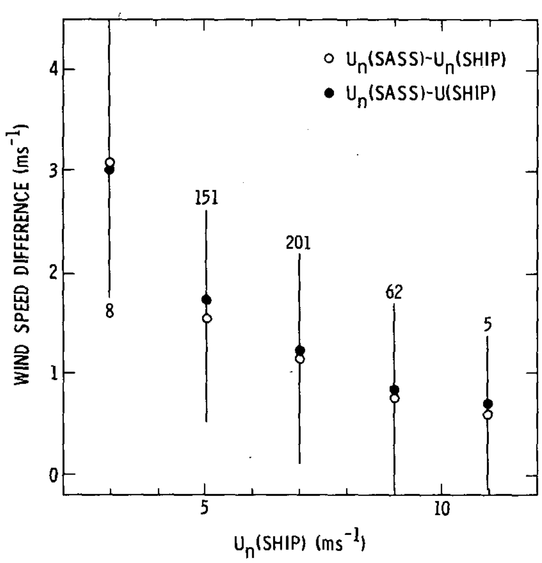


FIG. 5. Wind speed differences versus neutral winds from ship $U_n$ (ship). $U_n$ (SASS) is the SASS wind and $U$ (ship) is the observed wind from ship.

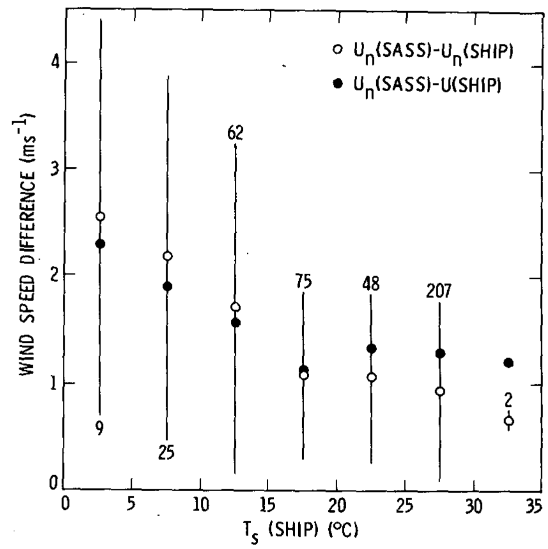


FIG. 6. As in Fig. 5 except versus sea surface temperature $T_s$.

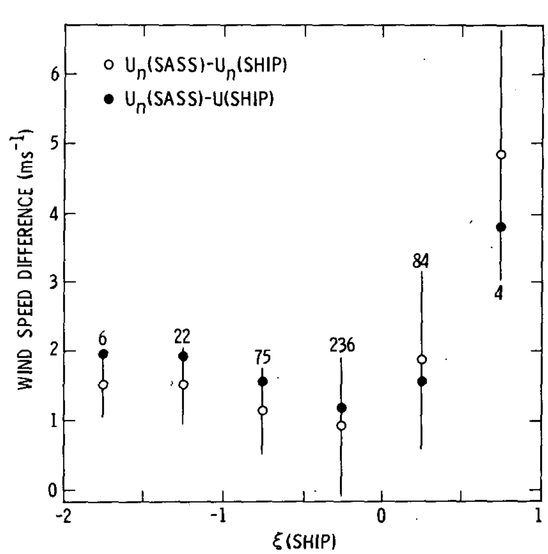


FIG. 7. As in Fig. 5 except versus stability parameter $\xi$.

buoy winds (always within ±0.5 m $s^{-1}$), it is unlikely that the discrepancy is entirely due to inaccuracies in the ship winds. The SASS winds were produced through a model function which was tuned with *in situ* measurements prepared for the SEASAT-JASIN Workshop. These *in situ* measurements from various wind sensors were corrected to agree with the Vector Averaging Wind Recorder (VAWR) on the moored buoy W2 because this is one of the very few sensors that recovered a full length record during the experiment. However, a subsequent study by Weller *et al.* (1983) reveals that the VAWR on W2 has nonlinear response and the measurements during JASIN are about 10% too high. This may account for part of the discrepancy. Wentz and Thomas (1984) also found that the SASS winds generated by the SEASAT project (those used in this study) are about 1 m $s^{-1}$ higher than those generated by a new model function they developed.

Figures 5–7 demonstrate also that $\delta U$ and $\delta U'$ varies systematically with 3 factors: $U_n$, $T_s$, and $\xi$. Attempts to use alternative formulations of $\psi$ in the determination of $\xi$, similar to attempts by LL, resulted only in slight shifts or compression of the abscissas in Fig. 7 without significantly altering the stability dependent trend. The 3 factors $U_n$, $T_s$ and $\xi$, however, are not independent of each other and Figs. 5–7 do not reveal the individual effect of each factor on $\delta U$ or $\delta U'$ irrespective of other factors. The stability parameter $\xi$ is parameterized in terms of $U$ (or $U_n$), $T_s$, and other factors. At high wind speeds, stability approaches neutral ($\xi = 0$). As wind speed decreases, the atmosphere becomes more stable or unstable (the absolute value of $\xi$ increases). Since $\delta U$ decreases as wind speed increases in Fig. 5, $\delta U$ is expected to increase away from neutral. In addition, as $T_s$ increases, atmospheric stability will go from stable to unstable ($\xi$ decreases) if other factors do not change. Since $\delta U$ decreases with increasing $T_s$ in Fig. 6, $\delta U$ is expected to increase with increasing $\xi$. Therefore, the systematic variation with $\xi$ in Fig. 7 may just be the effects of variations in $U_n$ and $T_s$. Any latitudinal dependence of wind speed may also show up as a relation between wind speed and sea surface temperature which will further complicate the picture. To separate the effects of the three factors, multivariate linear regressions were obtained and the data were re-examined for dependence on a factor after removal of the systematic dependence on the other factors.

It can be demonstrated mathematically that for a multivariate regression

$$y = \sum_{m=1}^{M} \beta_m x_m,$$

which relates an estimand $y$ to $M$ input estimators $x_m$; a regression coefficient $\beta_m$ represents the relation between $y$ and that part of $x_m$ that is uncorrelated to any other $M - 1$ estimators (Chelton, 1983). Thus, a multivariate regression can be used as a selective filter, extracting only the effect on the estimand of each estimator. Regression 1–5 in Table 1 shows the results of multivariate linear regressions of the form

$$\delta U = A + BU_n + CT_s + D\xi$$

where $A$, $B$, $C$, and $D$ are constant coefficients and $N$ is the number of averages used in the regressions. In Regression 6–8, neutral winds from ship reports are replaced by the observed winds. A nonzero coefficient indicates a dependence of the wind speed difference on the corresponding factor. The coefficients underlined are significantly different from zero with 90% of confidence if the $N$ data input are independent. The actual number of independent samples should be less than $N$. In Regression 1 and 6, the coefficients $B$, $C$, and $D$ indicate that $\delta U$ and $\delta U'$ decrease with increasing $U_n$, decrease with increasing $T_s$, but increase with increasing $\xi$. Since ship winds are likely to have systematic errors (instrument response and ship motion) that are larger at lower wind speeds, some of the systematic variation of $\delta U$ or $\delta U'$ in Fig. 5 and represented by the magnitude of coefficient $B$ may be due to systematic errors in ship winds. On the other hand, the accuracy of ship winds should not depend on $T_s$ or $\xi$. Addition of any one of the three variates to a regression on the other two always increases the correlation and decreases the rms scatter from the regression. This does not,

TABLE 1. Multivariate linear regressions of wind speed differences.

| Number | Regression | Condition | $A$ | $B$ | $C$ | $D$ | $N$ |
|---|---|---|---|---|---|---|---|
| 1 | $\delta U = A + BU_n + CT_s + D\xi$ | — | 5.65 | $\underline{-0.459}$ | $\underline{-0.0573}$ | $\underline{0.587}$ | 428 |
| 2 | $\delta U + A + BU_n + CT_s + D\xi$ | $U_n > 8$ | 5.63 | $\underline{-0.567}$ | 0.007 | 0.998 | 68 |
| 3 | $\delta U = A + BU_n + CT_s + D\xi$ | $U_n < 6$ | 7.22 | $\underline{-0.588}$ | $\underline{-0.103}$ | 0.290 | 159 |
| 4 | $\delta U = A + BU_n + CT_s + D\xi$ | $\xi < 0$ | 4.43 | $\underline{-0.341}$ | $\underline{-0.0473}$ | 0.160 | 340 |
| 5 | $\delta U = A + BU_n + CT_s + D\xi$ | $\xi > 0$ | 5.62 | $\underline{-0.451}$ | $\underline{-0.0735}$ | 2.285 | 88 |
| 6 | $\delta U' = A + BU + CT_s + D\xi$ | — | 5.10 | $\underline{-0.407}$ | $\underline{-0.0476}$ | 0.260 | 428 |
| 7 | $\delta U' = A + BU + CT_s + D\xi$ | $\xi < 0$ | 4.40 | $\underline{-0.331}$ | $\underline{-0.0424}$ | 0.0069 | 340 |
| 8 | $\delta U' = A + BU + CT_s + D\xi$ | $\xi > 0$ | 5.70 | $\underline{-0.472}$ | $\underline{-0.0730}$ | 1.333 | 88 |

however, necessarily imply increase in the precision of the estimate.

To examine the dependence more closely, the data are divided into subsets as specified in the third column of the table. Regressions 2 and 3 show that, for those data with $U_n$ higher than 8 m $s^{-1}$, the dependence on $T_s$, as indicated by the magnitude of $C$, is much smaller than that for data with $U_n$ smaller than 6 m $s^{-1}$. There is significant dependence of $T_s$ at low wind speeds but not at high wind speeds. When only unstable data are used, the coefficient $D$ in Regression 4 indicates a positive slope contradicting the plot in Fig. 7. The negative slope in the unstable regime in Fig. 7 is probably the effect of $U_n$ variation. The values of coefficient $D$ in Regressions 4–5 reveal that the effects of stability are much stronger under stable than unstable conditions. In both cases, however, the dependence is not significant at 90% level. When neutral winds from ship reports are replaced by the observed winds, as in Regression 6–8, the dependences on $U_n$ and $T_s$ do not change as much as the dependence on $\xi$. The stability dependences, as represented by the magnitude of $D$, are less in Regression 6–8 than those in Regression 1, 4, and 5, indicating that SASS winds may agree better with observed winds than with neutral winds. For the 428 averages, the correlation coefficient between $U_n$ (SASS) and $U_n$ (ship) is 0.70, less than the coefficient between the detrended $U_n$ (SASS) and $U$ (ship), which is 0.76. By examining whether the confidence intervals overlap, the coefficients are found to differ significantly with 80% confidence if at least 93% of the data are independent, but the difference is not significant with 90% confidence even if all the data are independent.

After $\delta U$ as represented by Regression 1 is removed from $U_n$ (SASS), the rms difference between $U_n$ (SASS) and $U_n$ (ship) is reduced from 1.7 m $s^{-1}$ to 0.9 m $s^{-1}$. Since the stability dependence is significantly reduced if the neutral winds are replaced by the actual winds, an alternative regression,

$$\delta U' = 4.96 - 0.38U - 0.5T_s,$$

was obtained and subtracted from $U_n$ (SASS). The rms difference between the resulting SASS winds and the observed ship winds is also about 0.9 m $s^{-1}$.

In order to help visualize these results, quadratic trends of $\delta U$ as functions of $U_n$ and $T_s$ were removed from $U_n$ (SASS) before the wind ratio $R = U_n$ (SASS)/$U_n$ (ship) was evaluated and plotted against $\xi$ in Fig. 8. In doing so, part of the stability dependence related to $U_n$ and $T_s$ are also removed. Despite this over-correction, the detrended data indicate that the ratio increases with stability independent of $U_n$ and $T_s$. The trend is stronger under stable than unstable conditions agreeing with the results shown in Table 1.

The 19.5 m wind speeds $U$ at various stabilities corresponding to a neutral 19.5 m wind $U_n$ of 7 m $s^{-1}$ were evaluated from the surface layer model of Liu *et al.* (1979). The theoretical ratio $U/U_n$ is plotted against

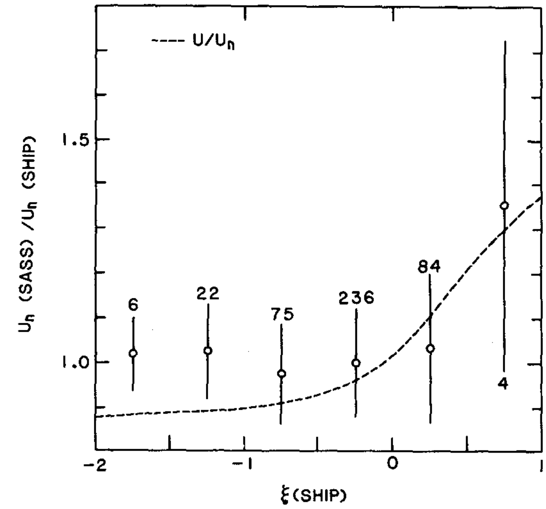


FIG. 8. The ratio of detrended SASS wind $U_n$ (SASS) to neutral wind from ship reports $U_n$ (ship) versus stability parameter $\xi$.

$\xi$ as dashed line in Fig. 8. The ratio $U/U_n$ depends only very slightly on $U_n$. The agreement between the data trend and the dashed curve in Fig. 8 suggests that SASS winds may agree better with observed winds than neutral winds from ship reports as demonstrated by the multivariate regressions. If the hypothesis that the amplitude of shortwaves is more closely related to surface stress than to surface wind is correct, $U_n$ (SASS) should correlate better with $U_n$ (ship) than with $U$ (ship) since $U_n$ (ship) is related directly to $U_*$ through the logarithmic relation. Furthermore, $U_n$ (SASS)/$U_n$ (ship) should show less stability dependence than $U_n$ (SASS)/$U$ (ship). Our results fail to support these two requirements.

With the continuation of the method used to obtain $R$ in Fig. 8, the quadratic trends of $\delta U$, as a function of $U_n$ and $\xi$, were removed from $U_n$ (SASS) before $R$ was plotted against $T_s$ in Figs. 9–11. Despite removal of part of the $T_s$ dependence related to $U_n$ and $\xi$, Figs. 9 and 10 show that $R$ decreases with increasing $T_s$. The trend is more pronounced at low wind speeds (Fig. 10). The dependence on $T_s$ decreases with increasing wind speed and, at wind speeds above 8 m $s^{-1}$, the trend almost disappears (Fig. 11).

According to the theory of Bragg scattering (Wright, 1968), $\sigma$ should be proportional to the spectral density of the short waves. Lleonart and Blackman (1980) suggested that the spectral density of capillary waves depends not only on $U_*$ but is also proportional to $(\nu/\gamma)^{0.5}$ where $\nu$ is the kinematic viscosity and $\gamma$ is the surface tension divided by density. Within the range of $T_s$ in this study, $\nu$ changes by almost 50% while $\gamma$ changes by only 5%, so the effect of surface tension due to temperature change can be neglected. It is assumed that the spectral density is proportional to $U_n{}^H\nu^{0.5}$, then

$$\sigma = KU_n{}^H\nu^{0.5},$$

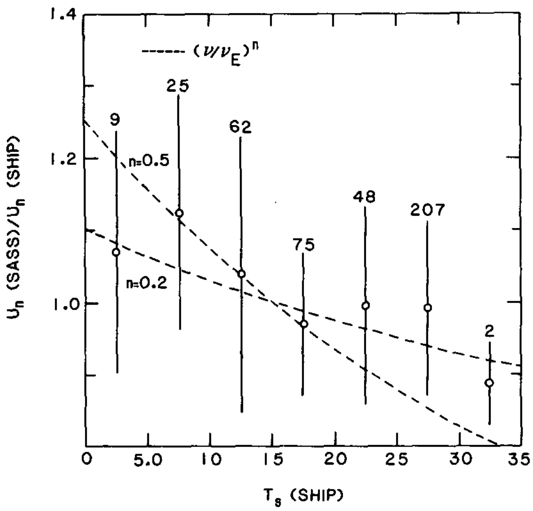


FIG. 9. As in Fig. 8 except versus sea surface temperature $T_s$.

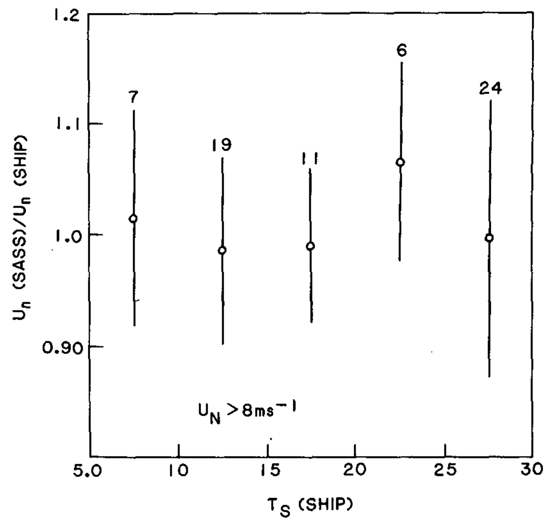


FIG. 11. As in Fig. 9 except for data with $U_n$ greater than 8 m s$^{-1}$ instead of all data.

where $K$ and $H$ are constants. The SASS model assumes

$$\sigma = GU_n^H,$$

where $G$ is a constant and it is equivalent to assume

$$G = K\nu_E^{0.5},$$

where $\nu_E$ is the kinematic viscosity at an equivalent temperature. The ratio of SASS wind to the correct neutral wind is then equal to $(\nu/\nu_E)^n$ where $n = 0.5/H$. The two curves in Fig. 9 correspond to $H = 1$ and $H = 2.5$ with $\nu_E$ at 15°C. Both the data and the theoretical curves decrease with increasing $T_s$.

The temperature dependence at low wind speeds exhibited by our data is consistent with the hypothesis of Lleonart and Blackman (1980) that the spectral density of capillary waves increases with viscosity. High turbulent intensity and wave breaking at high wind speeds may reduce the effect of viscosity and, therefore, the effects of temperature. However, the direct dependence of short waves on viscosity has not been clearly demonstrated. Different wind–wave relations have been observed on the surface of different fluids. Francis (1954) found that the wind speed at which short waves start to form is higher for oil than water but once waves start to form on oil they grow fast. Reduction of K-band microwave scatter over areas covered with surface films also has been observed (e.g., Huhnerfuss *et al.*, 1981; Johnson and Croswell, 1982). However, whether these changes are caused by viscosity or other fluid properties has not been resolved.

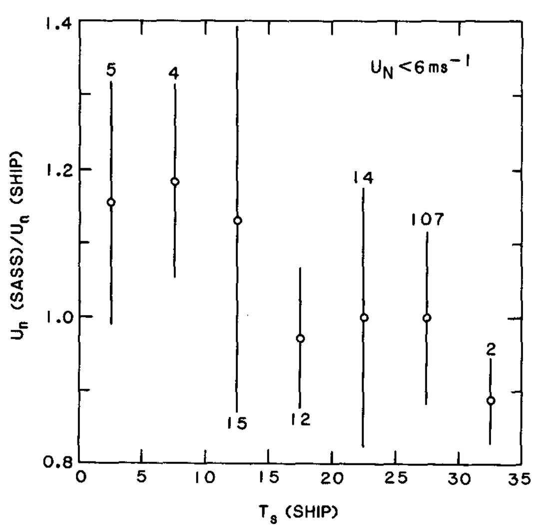


FIG. 10. As in Fig. 9 except for data with $U_n$ less than 6 m s$^{-1}$ instead of all data.

Only the analysis of the combined set of data from the two regions is shown. The same analysis on data from each region has been performed also, and the results are similar to those for the combined data. Meteorological and oceanic systems come in regimes. In estimating how representative the results are, the application of standard sampling theory is handicapped by the fact that the data are unevenly distributed in two-dimensional space and that not all the data in each sample are independent. However, the consistency of the results in two different regions (independent samples) increases the reliability of the results.

## 6. Conclusion

The average SASS winds are found to be generally higher than the average ship winds underscoring the importance of understanding the *in situ* measurements used to calibrate or validate SASS observations. This study identifies two factors, sea surface temperature and atmospheric stability, which affect microwave scatter and, therefore, wave development. In some cases, the effect may be small relative to the scatter of the data, but the consistent occurrence of these effects in all sets of data and for different analyzing methods demonstrates the reliability of the results.

The rms difference between the average SASS winds and ship winds is less than 2 m $s^{-1}$, the requirement specified for SASS (O'Brien, 1982). However, in some important applications, a greater accuracy is desirable. For example, Rasmusson and Carpenter (1982) showed that the maximum composite wind anomaly at eastern and central equatorial Pacific is about 4 m $s^{-1}$. An accuracy of 2 m $s^{-1}$ represents only 50% of the signal. Since atmospheric stability and sea surface temperature vary with space and time, the systematic dependence of SASS winds on these two factors should be removed before applying SASS winds to study wind forcing of ocean circulation.

This study also demonstrates the problem of relating satellite observations to a fictitious quantity like the neutral wind that has to be derived from *in situ* observations with models. The uncertainty associated with the derivation makes it difficult to identify the cause of the stability dependence of the SASS winds, whether it is calibration error or deficiency in physics. Over some areas of the study, the Labrador Sea and the California Coast, the atmosphere is so stable that the wind profile cannot be predicted and the concept of neutral wind as used in the SASS model function should not be applied.

This study demonstrates also the dependence of SASS winds on sea surface temperature at low wind speeds, possibly due to temperature-dependent factors such as water viscosity, which affects wave development. The temperature dependence exhibited by our data is consistent with the hypothesis of Lleonart and Blackman (1980) on capillary wave spectra. However, a controlled experiment that will isolate the viscosity effects on wave amplitude is needed for clarification. High turbulent intensity and wave breaking may reduce the effects of these factors and therefore the dependence on sea surface temperature at wind speeds above 8 m $s^{-1}$. The average wind speeds over considerable areas of this study are less than 8 m $s^{-1}$ as shown in Fig. 4, and the effects of sea surface temperature should be accounted for in global application of SASS winds.

Since the effects of wind, stability and surface temperature are related as discussed, the problem of isolating individual effects should be considered carefully in future experiments. The observations of Weissman *et al.* (1980) of sudden changes in radar backscatter at the boundary of the Gulf Stream is, most likely, due to a combination of causes: surface current, surface tension, viscosity, atmospheric stability and others. Some other important effects, such as natural or artificial surface films have not been examined in this study. The future challenge lies in identifying those factors that would significantly affect the relation between backscatter and surface wind-stress and parameterizing these effects in terms of satellite observations.

*Acknowledgments.* This study was performed at the Jet Propulsion Laboratory, California Institute of Technology, under contract with National Aeronautic and Space Administration. The author is grateful to Steve Pazan who helped to acquire the ship reports and gave valuable suggestions in processing these ship data. Jeff Hilland kindly advised on the Pilot Ocean Data System where most of the data processing was conducted. Discussions with colleagues Peter Woiceshyn, Frank Carsey, Dudley Chelton and Robert Stewart through the course of this study were also helpful.

REFERENCES

Boggs, D. H., 1982: SEASAT scatterometer geophysical data record (GDR) users handbook, Intern. Rep. 622-232, Jet Propulsion Lab. 39 pp.

Brown, R. A., 1983: On a satellite scatterometer as an anemometer. *J. Geophys. Res.*, **88**, 1663–1673.

Chelton, D. B., 1983: Effects of sampling errors in statistical estimation. *Deep-Sea Res.*, **30**, 1083–1103.

——, and J. J. O'Brien, 1982: Satellite microwave measurements of surface wind speed in the Tropical Pacific. *Trop. Ocean-Atmos. Newslett.*, **11**, 2–4.

Ching, J. K. S., 1976: Ship's influence on wind measurements determined from BOMEX mast and boom data. *J. Appl. Meteor.*, **15**, 102–106.

Esbensen, S. K., and R. W. Reynolds, 1981: Estimating monthly averaged air–sea transfers of heat and momentum using bulk aerodynamic methods. *J. Phys. Oceanogr.*, **11**, 457–465.

Francis, J. R. D., 1954: Wave motions and the aerodynamic drag on a free oil surface. *Philos. Mag.*, **45**, 695–702.

Huhnerfuss, H., W. Alpers, W. L. Jones, P. A. Lange and K. Richter, 1981: The damping of ocean surface waves by a monomolecular film measured by wave staffs and microwave radars. *J. Geophys. Res.*, **86**, 429–438.

Ishimaru, A., 1978: *Wave Propagation and Scattering in Random Media, Vol. 2.* Academic Press, 570 pp.

Johnson, J. W., and W. F. Croswell, 1982: Characteristics of 13.9 GHz radar scattering from oil film in the sea surface. *Radio Sci.*, **17**, 611–617.

Jones, W. L., L. C. Schroeder, D. H. Boggs, E. M. Bracalente, R. A. Brown, G. J. Dome, W. J. Pierson and F. J. Went, 1982: The SEASAT-A satellite scatterometer: The geophysical evaluation of remotely sensed wind vectors over the ocean. *J. Geophys. Res.*, **87**, 3297–3317.

Liu, W. T., and W. G. Large, 1981: Determination of surface stress by SEASAT-SASS: A case study with JASIN data. *J. Phys. Oceanogr.*, **11**, 1603–1611.

——, and K. B. Katsaros, 1984: Analysis of sea surface and air temperature measured from aircraft in the Joint Air Sea Interaction (JASIN) experiment. Submitted to *J. Geophys. Res.*

——, —— and J. A. Businger, 1979: Bulk parameterization of air–sea exchanges of heat and water vapor including the molecular constraints at the interface. *J. Atmos. Sci.*, **36**, 1722–1735.

Lleonart, G. T., and D. R. Blackman, 1980: The spectral characteristics of wind-generated capillary waves. *J. Fluid Mech.*, **97**, 455–479.

O'Brien, J. J., 1982: *Scientific Opportunities Using Satellite Wind Stress Measurements over the Ocean, Report of the Satellite Surface Stress Working Group.* Nova University/N.Y.I.T. Press, 153 pp.

Phillips, O. M., 1977: *The Dynamics of Upper Ocean.* Cambridge University Press, 336 pp.

Pierson, W. J., 1983: The measurement of the synoptic scale wind over the ocean. *J. Geophys. Res.*, **88**, 1683–1708.

Rasmusson, E. M., and T. H. Carpenter, 1982: Variations in tropical sea surface temperature and surface wind fields associated with Southern Oscillation/El Nino. *Mon. Wea. Rev.*, **110**, 354–384.

Schroeder, L. A., *et al.*, 1982: The relationship between wind vector and normalized radar cross sections used to derive SEASAT-A satellite scatterometer winds. *J. Geophys. Res.*, **87**, 3318–3336.

Thompson, T. W., W. T. Liu and D. E. Weissman, 1983: Synthetic aperture radar observation of ocean roughness from rolls in unstable marine boundary layer. *Geophys. Res. Lett.*, **10**, 1172–1175.

Weissman, D. E., T. W. Thompson and R. Legeckis, 1980: Modulation of sea surface radar cross sections by surface stress: Wind speed and temperature effects across the Gulf Stream. *J. Geophys. Res.*, **85**, 5032–5042.

Weller, R. A., R. E. Payne, W. G. Large and W. Zenk, 1983: Wind measurements from an array of oceanographic moorings and from F. S. Meteor during JASIN 1978. *J. Geophys. Res.*, **88**, 9689–9705.

Wentz, F. J., and L. A. Thomas, 1984: A model function for ocean radar cross sections at 14.6 GHz. Submitted to *J. Geophys. Res.*

Wright, J. W., 1968: A new model of sea clutter. *IEEE Trans. Antennas Propag.*, **AP-16**, 217–223.

Wurtele, M. G., P. M. Woiceshyn, S. Peteherych, M. Borowski and W. S. Appleby, 1982: Wind direction alias removal studies of SEASAT scatterometer-derived wind fields. *J. Geophys. Res.*, **87**, 3365–3377.